AIP | Review of Scientific Instruments

Diagnostics for molybdenum and tungsten erosion and transport in NSTX-U

F. Scotti, V. A. Soukhanovskii, and M. E. Weller

Citation: Review of Scientific Instruments **87**, 11D445 (2016); doi: 10.1063/1.4963146
View online: http://dx.doi.org/10.1063/1.4963146
View Table of Contents: http://scitation.aip.org/content/aip/journal/rsi/87/11?ver=pdfcov
Published by the AIP Publishing

Diagnostics for molybdenum and tungsten erosion and transport in NSTX-U

F. Scotti, V. A. Soukhanovskii, and M. E. Weller
Lawrence Livermore National Laboratory, Livermore, California 94551, USA

(Presented 6 June 2016; received 7 June 2016; accepted 2 September 2016;
published online 13 October 2016)

A comprehensive set of spectroscopic diagnostics is planned in the National Spherical Torus Experiment Upgrade to connect measurements of molybdenum and tungsten divertor sources to scrape-off layer (SOL) and core impurity transport, supporting the installation of high-Z plasma facing components which is scheduled to begin with a row of molybdenum tiles. Imaging with narrow-bandpass interference filters and high-resolution spectroscopy will be coupled to estimate divertor impurity influxes. Vacuum ultraviolet and extreme ultraviolet spectrometers will allow connecting high-Z sources to SOL transport and core impurity content. The high-Z diagnostics suite complements the existing measurements for low-Z impurities (carbon and lithium), critical for the characterization of sputtering of high-Z materials. *Published by AIP Publishing.* [http://dx.doi.org/10.1063/1.4963146]

I. INTRODUCTION

The National Spherical Torus Experiment Upgrade (NSTX-U) is planning a transition from graphite (ATJ-grade and POCO) plasma facing components (PFCs) to a full high-Z metallic PFCs coverage. The PFCs progression, which is to occur over the next 5-10 years,[1] will start with the replacement of a row of graphite tiles (second tile row of the outer lower divertor) with TZM (titanium-zirconium-molybdenum)-alloy molybdenum tiles. A castellated surface design with chamfered edges will be employed to mitigate the thermo-mechanical stresses. Two of the ninety six high-Z tiles will be made of tungsten to inform future decisions on the materials for the high-Z PFC progression.

The progressive transition to a full high-Z wall will require studying the distribution of impurity sources and their role in core contamination. A source at a single poloidal location represents an ideal setup for the determination of the transport processes connecting divertor sources to core impurity inventory, including gross and net divertor influxes, scrape-off layer (SOL) parallel transport, and core radial transport.[2]

A comprehensive suite of spectroscopic diagnostics is being developed in NSTX-U to study the high-Z impurity transport chain. Imaging with narrow-bandpass interference filters and high-resolution spectroscopy will be coupled to estimate gross and net divertor impurity influxes. Vacuum ultraviolet (VUV) and extreme ultraviolet (EUV) spectrometers will allow the connection of high-Z sources with SOL transport and core impurity content. The EUV spectrometers combined with measured divertor impurity influxes will enable the determination of impurity core penetration efficiencies and confinement times in different operational scenarios. The NSTX-U diagnostic suite for high-Z impurity sources and transport is described in the remainder of the paper.

Note: Contributed paper, published as part of the Proceedings of the 21st Topical Conference on High-Temperature Plasma Diagnostics, Madison, Wisconsin, USA, June 2016.

II. DIAGNOSTICS FOR HIGH-Z DIVERTOR SOURCES

Ultraviolet (UV) and visible spectroscopy are commonly used to measure gross erosion of high-Z (Mo, W) materials in fusion devices.[3–5] Spectrally unresolved measurements (filterscopes[6] and two-dimensional (2D) filtered imaging[7]) of low intensity emission lines proved to be more complicated due to the comparable contribution from line and continuum emission (due to visible Bremsstrahlung, molecular, and Planck emission). To deal with this problem, a narrow-bandpass filtered intensified charge-injection-device (CID) camera was used in Alcator C-Mod, subtracting the continuum contribution from repeated discharges[7] while a cross-calibration of filtered photomultiplier tubes and spectrometer measurements was used at JET.[6] The approach chosen on NSTX-U for the measurement of high-Z impurity influxes is to couple CID cameras and dual-spectral imaging via the TWICE (Two-Wavelength Imaging Camera Equipment) systems.[8] TWICE combines 2D imaging via an image-intensified radiation-hardened CID camera (ThermoScientific CID8710D1M camera, Photonis GENII-UV intensifier) with beam-splitting optics, to synchronously image the same field of view at two different wavelengths. The 2D imaging allows the evaluation of toroidal variations in impurity erosion (in addition to its radial profile), such as due to the presence of leading edges. The two-wavelength capability enables the real-time subtraction of the continuum contribution on the same field of view. The detector has a 720×480 pixel resolution with 8 bit digitization on 30 Hz interlaced frames (effective time resolution of 16 ms). The photocathode of the image intensifier has a quantum efficiency (QE) of 17%, 19%, and 6% at 200, 400, and 600 nm, respectively. The remote control of intensifier gate timing and width will enable edge-localized-mode (ELM)-resolved 2D erosion imaging, syncing to externally triggered ELMs. Molybdenum erosion will be measured, as done in Alcator C-Mod,[7] via the 550.8 nm Mo I transition ($4d^5 5s$–$4d^5 5p$). However, unlike in Alcator C-Mod the continuum contribution will be monitored at longer wavelengths (551.5 nm) due to the presence of a Li II transition at 548.5 nm.

Measurements of neutral tungsten influxes are expected to be more challenging than molybdenum, due to the lower sputtering yields[9] and to the larger inverse photon efficiency S/XB for the neutral tungsten visible transitions.[10] A higher throughput TWICE system, TWICE-II, was therefore implemented exploiting the light throughput (2.5×) of a larger coherent fiber bundle (Schott IG-163 8 × 10 mm versus Schott IG-154 4 × 4 mm) and 2-in. aperture optics. Additionally, a CID camera with stronger intensification (10^6 versus $\sim 3 \times 10^3$) was assigned to TWICE-II (ThermoScientific CID3710D1M camera, Photonis XX1450-UV intensifier), enabling the imaging of even weaker emission lines. The photocathode of the image intensifier has a QE of 28%, 20%, and 8% at 200, 400, and 600 nm, respectively. Tungsten will be monitored via the commonly used 400.9 nm transition ($5d^5 6s$–$5d^5 6p$) and the nearby continuum will be monitored at 401.5 nm.

The two TWICE systems have comparable fields of view (~30° toroidally, ~50 cm radially) of the lower divertor, are separated by 30° toroidally, and have a spatial resolution of ~1 mm/pixel. The TWICE-II field of view is centered toroidally at the location of the tungsten tiles. Both systems are currently operational in NSTX-U and dedicated to the monitoring of other emission lines: O II (filter central wavelength λ_0 = 441.6 nm, full width at half maximum FWHM $\Delta\lambda$ = 1.3 nm), B II (λ_0 = 703.0 nm, $\Delta\lambda$ = 5.0 nm), CD Gerö band (λ_0 = 429.5 nm, $\Delta\lambda$ = 3.0 nm), D-γ (λ_0 = 433.9 nm, $\Delta\lambda$ = 1.2 nm). The field of view of the two cameras and the diagnostic layout in the NSTX-U poloidal cross section are shown in Figures 1 and 2, respectively. The future location of the high-Z tiles is indicated with an arrow in Figure 1. An image from TWICE-I from a NSTX-U plasma discharge with strike point at the location of the future high-Z tiles is shown in Figure 1(c), as imaged though D-γ and O II filters.

The capabilities of the imaging systems are augmented by a high resolution UV-VIS-NIR (ultraviolet-visible-near infrared) spectrometer DIMS[11] with dedicated lines of sight on molybdenum and tungsten tiles. DIMS will allow the spectrally resolved monitoring of neutral molybdenum and tungsten transitions and the evaluation of net erosion rates via measurement of Mo II and W II emission lines in the UV spectral range.[12] The DIMS temporal resolution (~2 ms) will enable ELM-resolved measurements of net erosion fluxes. Net erosion rates are to be compared with the gross erosion measured by the TWICE systems for an estimate of the impurity re-deposition fraction[5] and of the effective divertor impurity source. In addition, benchmark of S/XB coefficients is envisioned comparing influxes from Mo I transitions at 386 and 414 nm to measurements simultaneously performed with imaging systems at 550 nm.

Experience in ASDEX-Upgrade[4] and JET[5] demonstrated that inter-ELM high-Z erosion was dominated by sputtering from the main intrinsic impurity (carbon in ASDEX and beryllium in JET) while intra-ELM high-Z erosion was due to sputtering from high energy deuterium ions.[6] In particular, measuring/modeling the absolute low-Z impurity incident fluxes and their charge distribution in proximity of the target is needed to understand the measured effective high-Z sputtering yields. Simultaneous measurement of low-Z and high-Z impurity emission is therefore critical in the NSTX-U mixed-material environment originating from the use of different tile materials (graphite and high-Z) and conditioning methods (boronization, lithium evaporation). Spectroscopic diagnostics for high-Z impurity emission are complemented by the extensive low-Z impurity (Li, B, C, O) measurements in NSTX-U[13] performed via a combination of two-dimensional wide-angle bandpass-filtered fast cameras and filtered line-scan cameras. Available filters include C I-IV, Li I-II, O II, B II and will enable studying the role of carbon migration and deposition onto high-Z tiles in controlling the effective high-Z sputtering yield, and characterizing lithium behavior (coating longevity, fuel recycling, and oxygen gettering) on high-Z versus graphite substrates.

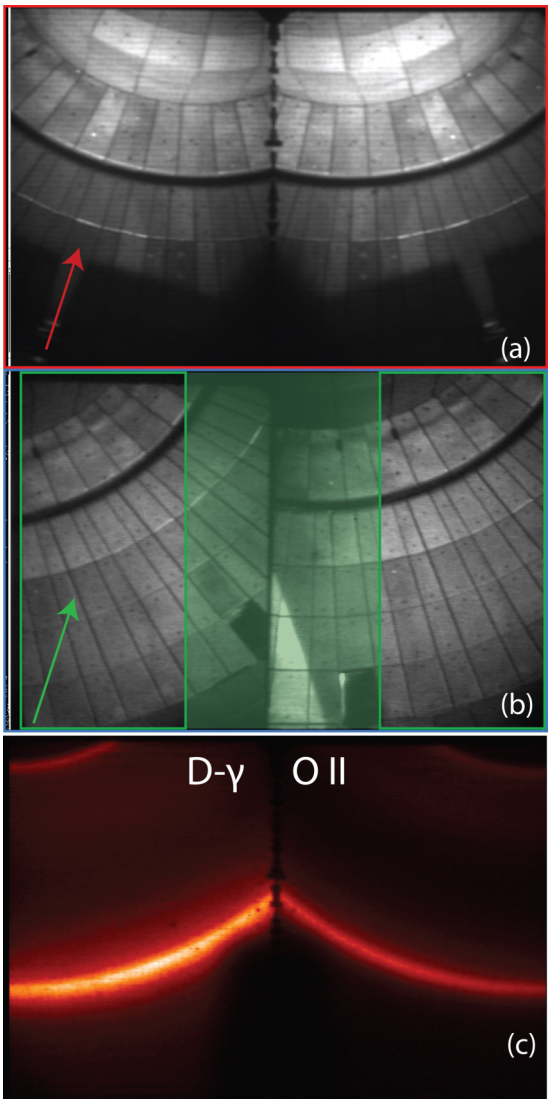

FIG. 1. NSTX-U lower divertor tiles as imaged via TWICE-I (a) and TWICE-II (b). Location of the future high Z tile is shown with arrows. Image from TWICE-I (c) from a NSTX-U plasma discharge with strike point at the location of the future high-Z tiles, as imaged though D-γ and O II filters.

III. DIAGNOSTICS FOR SOL AND CORE TRANSPORT

SOL parallel transport and core radial transport are responsible for the core penetration and accumulation of

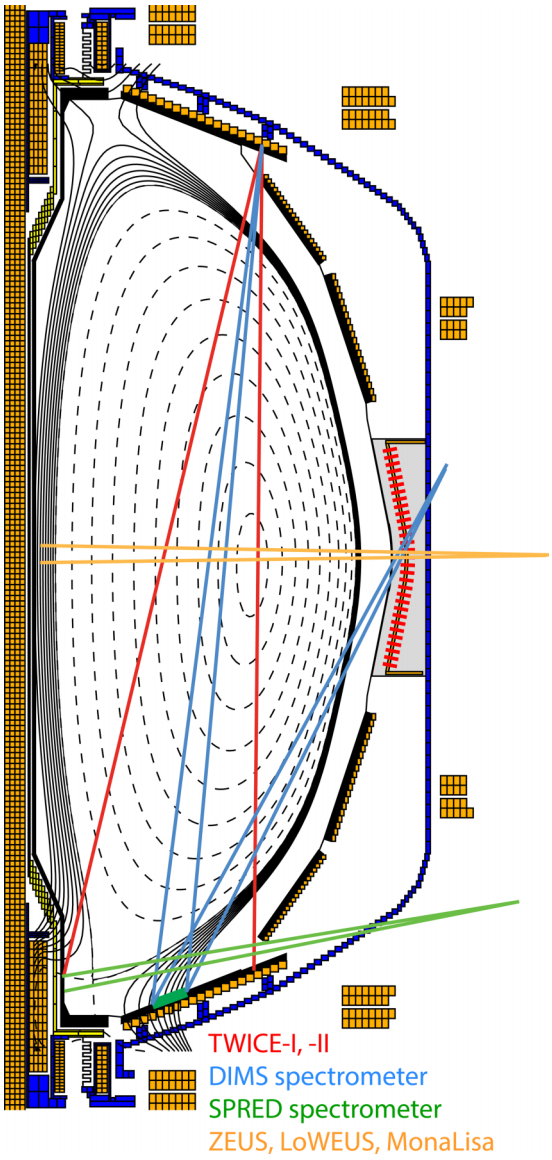

FIG. 2. Poloidal cross section of the NSTX-U vacuum vessel with an equilibrium reconstruction of a high-triangularity plasma. Field of view of TWICE systems and lines of sight of DIMS, SPRED, and core EUV spectrometers are indicated in red, blue, green, and orange, respectively.

divertor sources. VUV and EUV spectrometers will allow connecting high-Z sources with SOL and core impurity content in NSTX-U.

A divertor VUV SPRED (survey, poor resolution, extended domain) spectrometer (McPherson Model 251, flat-field, 0.3 m) will be installed in NSTX-U[14] with a single line of sight aimed at the outer divertor leg, enabling studies of charge state distribution and transport along the divertor leg. The NSTX-U divertor SPRED covers the spectral range between 200 Å and 1600 Å, imaged via a micro-channel plate and a Schott coherent imaging bundle (25×4 mm) onto a Princeton Instruments ProEM CCD camera (1600×200 pixels) with read-out times as low as 0.7 ms in full-binning mode. In this wavelength range, the expected molybdenum charge states for T_e values characteristic of the NSTX-U divertor region include Mo III to Mo XIV.[15] Relative changes in intermediate molybdenum charge states with respect to gross and net divertor influxes will allow qualitative understanding of divertor retention of high-Z sources. Multi-fluid modeling is envisioned to aid in the interpretation of the SPRED data via T_e and charge state distribution along the divertor leg.

A suite of three EUV flat-field grazing-incidence core spectrometers XEUS, LoWEUS, and MonaLisa[16] is currently installed in NSTX-U and provides measurements of low and high Z core impurity emission. The three spectrometers provide spectral coverage of 8-65 Å, 50-220 Å, 190-450 Å, respectively. XEUS uses a 2400 lines/mm grating at 3° incidence with a spectral resolution of 0.1 Å in FWHM. LoWEUS and MonaLisa both use a 1200 lines/mm grating at 1.3° incidence with a 0.3 Å resolution. All the spectrometers have a 100 μm slit and a Princeton Instruments PIXIS-XO 100B CCD detector (1300×100 pixels, 20 μm). The EUV spectrometers are installed at the same toroidal location on the NSTX-U vacuum vessel with a single cord looking radially at the core plasma, as indicated in Figure 2. The time resolution of the spectrometers is of 5 ms, enabling studies of temporal evolution of impurity content. Given the typical T_e values observed in the NSTX-U core plasma (0.1-1.5 keV), Mo XVI–Mo XXIII and W XXVIII–W XLIV transitions are expected in the spectral range covered by the EUV spectrometers. The relative changes in the EUV line brightness from molybdenum and tungsten, combined with measured divertor impurity influxes, will enable estimates of relative changes in impurity core penetration efficiencies and confinement times in different operational scenarios. The combination of the EUV spectrometers with high-Z perturbative studies with the Laser Blow Off (LBO) system[16] will allow the comparison of penetration efficiencies between divertor and midplane sources, evaluating the change in core impurity content relative to the measured absolute sources from the divertor and the LBO system. Possible differences in impurity penetration factors will inform decisions on the progression of the PFC materials upgrade in NSTX-U.

ACKNOWLEDGMENTS

This work was supported by U.S. DOE Contract Nos. DE-AC02-09CH11466 and DE-AC52-07NA27344. The digital data for this paper can be found in http://arks.princeton.edu/ark:/88435/dsp018p58pg29j.

[1]NSTX-U Five Year Plan for FY2014-2018, http://nstx-u.pppl.gov/five-year-plan/five-year-plan-2014-18.
[2]P. Stangeby, *The Plasma Boundary of Magnetic Fusion Devices* (Institute of Physics Publishing, Bristol, 2000).
[3]B. Lipschultz *et al.*, Nucl. Fusion **41**, 585 (2001).
[4]R. Dux *et al.*, J. Nucl. Mater. **390-391**, 858 (2009).
[5]G. vanRooij *et al.*, J. Nucl. Mater. **438**, S42 (2013).
[6]N. D. Harder *et al.*, Nucl. Fusion **56**, 026014 (2016).
[7]A. James *et al.*, Plasma Phys. Controlled Fusion **55**, 125010 (2013).
[8]F. Scotti *et al.*, Rev. Sci. Instrum. **86**, 123103 (2015).
[9]W. Eckstein *et al.*, Nucl. Fusion (Suppl.) - At. Plasma-Mater. Interact. Data Fusion **1**, 51 (1991).
[10]H. P. Summers, The ADAS User Manual, version 2.6, http://www.adas.ac.uk (2004).
[11]V. Soukhanovskii *et al.*, Rev. Sci. Instrum. **81**, 10D723 (2010).
[12]S. Loch, private communication (2015).
[13]F. Scotti *et al.*, Rev. Sci. Instrum. **83**, 10E532 (2012).
[14]V. A. Soukhanovskii *et al.*, Rev. Sci. Instrum. **87**, 11D605 (2016).
[15]M. Finkenthal *et al.*, Phys. Lett. A **82**, 123 (1981).
[16]M. E. Weller *et al.*, Rev. Sci. Instrum. **87**, 11E324 (2016).